DOI: 10.1002/ejic.200801151

Carbon–Silicon Bond Activation by [Pd(I*t*Bu)$_2$] – the Molecular Structures of [Pd(Me$_3$Si)(I*t*Bu)(μ-I)]$_2$ and [Pd(CH$_2$I*t*Bu)I$_2$]

Oriana Esposito,[a] Deborah E. Roberts,[a] F. Geoffrey N. Cloke,*[a] Stephen Caddick,*[b] Jennifer C. Green,*[c] Nilay Hazari,[c] and Peter B. Hitchcock[a]

Keywords: Palladium / N-heterocyclic carbenes / Oxidation / Zwitterions / Density functional calculations

The reaction of Me$_3$SiCH$_2$I with [Pd(I*t*Bu)$_2$] (I*t*Bu = 1,3-di-*tert*-butyl-imidazol-2-ylidene) results, not in simple oxidative addition, but in carbon–silicon bond activation and formation of [Pd(Me$_3$Si)(I*t*Bu)(μ-I)]$_2$ (**2**) and [Pd(CH$_2$I*t*Bu)I$_2$] (**3**). The zwitterionic nature of the latter has been confirmed by DFT studies, and a possible mechanism for the formation of these two unexpected products is presented. Complex **2** has also been synthesised independently by the direct oxidative addition of Me$_3$SiI to [Pd(I*t*Bu)$_2$].

Introduction

The oxidative addition of halocarbons to transition-metal complexes has been extensively reported and is supported by a wealth of structural evidence.[1] In contrast, relatively few examples of the oxidative addition of silicon–halide bonds to transition-metal centres have been described.[2] Recently, the reactivity of molecules containing metal–silicon bonds has attracted considerable attention owing to their importance in a number of stoichiometric and catalytic transformations.[3] The studies conducted in this field have allowed a comparison with related systems containing a metal–carbon bond and provided a better understanding of the elementary steps in important industrial catalytic reactions, such as hydrosilylation,[4] dehydrogenative couplings of primary or secondary silanes,[5] silylformylation,[6] preparation of polysilanes[7] and bis-silylation.[8] Silylpalladium complexes are believed to be key intermediates in a number of such Pd-catalysed transformations, and the limited stability and the high reactivity of the Si–Pd bond in these compounds is believed to be responsible for their high catalytic activity. In fact, only a few stable complexes containing a Pd–Si bond have been isolated, particularly in the case of non-chelating systems.[9] [Pd(SiCl$_3$)$_2$(PPh$_3$)$_2$] has been obtained by the reaction of Pd(PPh$_3$)$_4$ with HSiCl$_3$ or Cl$_3$SiSiCl$_3$, and stable bis(silyl)palladium(II) complexes have been synthesised by the reaction of Pd^0 or Pd^{II} triphenylphosphane complexes with chelating hydrosilanes.[9c] Secondary hydrosilanes can also afford bis(silyl)-palladium(II) complexes, stabilised by bulky chelating phosphane ligands, e.g. [Pd(Cy$_2$PCH$_2$CH$_2$PCy$_2$)(SiMe$_2$H)$_2$].[9d]

Oxidative addition of TMSI to a palladium(0) catalyst to give a silylpalladium iodide intermediate, which undergoes insertion of alkyne into the Pd–Si bond, followed by transmetallation with an organostannane and reductive elimination of the coupled product has been described.[10] However, despite the key role of silylpalladium iodide intermediates in this transformation, no examples of stable L$_n$Pd(SiR$_3$)I type complexes have been reported.

We have been exploring reactivity of alkyl halides towards [Pd(NHC)$_2$] (NHC=N-heterocyclic-carbene) complexes, in the context of alkyl amination and have reported the indirect synthesis of dimers of the type [Pd(NHC)(neopentyl)(μ-Cl)]$_2$.[11] Given the unreactivity of neopentyl halides towards direct oxidative addition to Pd(NHC)$_2$,[11] we were interested to examine the more reactive silicon analogue Me$_3$SiCH$_2$I in this context, and also direct oxidative addition of trimethylsilyl halides to [Pd(NHC)$_2$].

Results and Discussion

Synthetic and Structural Studies

An excess of (trimethylsilyl)methyl iodide was treated with [Pd(I*t*Bu)$_2$] (I*t*Bu = 1,3-bis-*tert*-butyl-imidazol-2-ylidene) (**1**) at room temperature in benzene (Scheme 1) and filtered from palladium black. After several days, yellow and red crystals appeared on the walls of the reaction vessel. Subsequent single-crystal X-ray analysis revealed the molecular structure of the two reaction products (**2** and **3**), which are shown in Figures 1 and 2, respectively. The reac-

[a] Department of Chemistry and Biochemistry, School of Life Sciences, University of Sussex,
Falmer, Brighton BN1 9QJ, UK
E-mail: f.g.cloke@sussex.ac.uk
[b] Department of Chemistry, University College London,
20 Gordon Street, London WC1H 0AJ, UK
[c] Department of Chemistry, Oxford University, Inorganic Chemistry Laboratory,
South Parks Road, Oxford OX1 3QR, UK

tion of **1** with (trimethylsilyl)methyl iodide was reproduced several times, and always yielded **2** and **3** as co-crystallising products. Unfortunately, the very poor solubility of the two compounds in most solvents, and the ineffectiveness of sublimation as a separation technique in this case, did not allow the full characterisation of **3**. Compound **2**, however, was synthesised independently by a different route and fully characterised (vide infra).

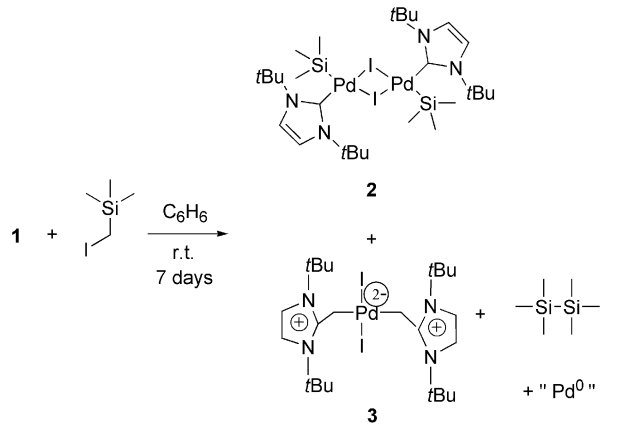

Scheme 1. Oxidative addition of (trimethylsilyl)methyl iodide to **1**.

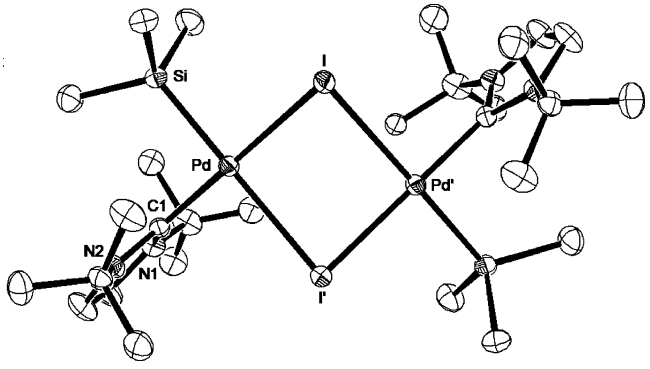

Figure 1. ORTEP diagram of [{(TMS)Pd(I*t*Bu)I}$_2$], **2**. Hydrogen atoms are omitted for clarity. Selected bond lengths [Å] and angles [°]: Pd–C(1) 2.017(6), Pd–Si 2.3155(18), Pd–I 2.6496(6), Pd–I′ 2.8759(6); C(1)–Pd–Si 89.80(16), C(1)–Pd–I 179.9(2), Si–Pd–I 90.17(5).

[(I*t*Bu)Pd(TMS)(μ-I)]$_2$ (**2**) exhibits the expected square-planar geometry, with the two *N*-heterocyclic carbene ligands coplanar and *trans*, and orthogonal to the central IPdI′ plane. The Pd–Si bond length [2.3155(18) Å] is comparable to that found in [*trans*-Pd(SiF$_2$Ph)(Cl)(PMe$_2$Ph)$_2$] [2.2680(6) Å][12] but shorter than those in [*trans*-Pd(Cab^{P,Si})$_2$] {Cab^{P,Si} = η^2-[(SiMe$_2$)(PR$_2$)C$_2$B$_{10}$H$_{10}$-*P,Si*]} [2.358(2)–2.361(2) Å][9h] and [Pd(dcpe)(SiMe$_3$)$_2$] {dcpe = 1,2-bis(dicyclohexylphosphanyl)ethane} (2.3561 Å),[9e] presumably because of the *trans* influence of the phosphane ligands in the two latter complexes relative to that of the halide ligands in **2** and [*trans*-Pd(SiF$_2$Ph)(Cl)(PMe$_2$Ph)$_2$].

The isolation of **2** as one of the products of the reaction of **1** with (trimethylsilyl)methyl iodide suggested the possibility of synthesising **2** by direct oxidative addition of

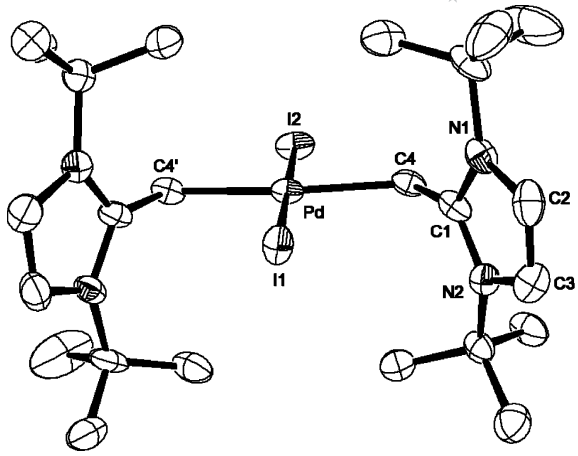

Figure 2. ORTEP diagram of [Pd(CH$_2$I*t*Bu)I$_2$].C$_6$H$_6$, **3**. Solvent molecules and hydrogen atoms are omitted for clarity. Selected bond lengths [Å] and angles [°]: Pd–I(1) 2.676(2), Pd–I(2) 2.635(2), Pd–C(4) 2.158(13), C(1)–C(4) 1.446(18), C(3)–C(2) 1.35(2); I(1)–Pd–C(4)′ 95.6(3), C(4)–Pd–I(2) 84.4(3), C(4)–Pd–C(4)′ 168.8(6), I(1)–Pd–I(2) 180.0(3).

trimethylsilyl iodide (TMSI) to **1**. Indeed, as shown in Scheme 2, the reaction of **1** with two equivalents of TMSI at room temperature over an extended period of time resulted in quantitative (as determined by NMR spectroscopy) formation of **2** and the imidazolium salt **4**, the latter arising from the reaction of dissociated I*t*Bu and the highly reactive TMSI.

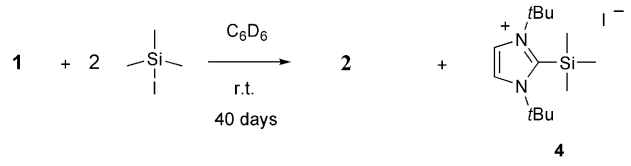

Scheme 2. Rational synthesis of **2**.

Although [Pd(CH$_2$I*t*Bu)$_2$I$_2$] (**3**) also exhibits the typical square-planar geometry about palladium with the two CH$_2$I*t*Bu ligands mutually *trans*, the electronic structure and bonding in **3** is clearly unusual. The zwitterionic Lewis structure shown in Scheme 1, in which a positive charge is delocalised in the π system of each N-heterocyclic ring and a double negative charge is localised on palladium, leads to a formal palladium oxidation state of II and thus seems reasonable. In order to explore the bonding in **3**, a DFT study was carried out.

Computational Studies

N-Methyl-substituted compound **5** (Figure 3) was used as a model for compound **3**, and a geometry optimisation was performed with no symmetry restrictions. The geometry was optimised to a structure with C_{2v} symmetry, conse-

quently the MOs are labelled according to their characters in this symmetry group. Important calculated bond lengths and angles are compared with the experimental values in Table 1.

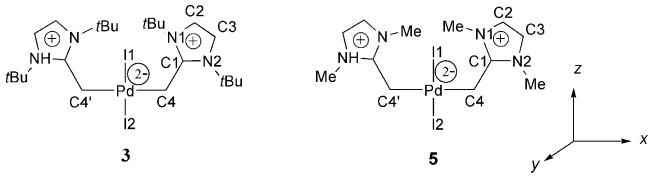

Figure 3. *N*-methyl-substituted compound **5**, used as a model for **3**. The atom labelling scheme for both compounds are shown.

Table 1. Comparison between selected experimental and calculated bond lengths [Å] and angles [°] in **3** and **5**.

Bond length or angle	Experimental values for **3**	Calculated values for **5**
Pd–I(1)	2.676(2)	2.63
Pd–I(2)	2.635(2)	2.62
Pd–C(4)	2.158(13)	2.12
C(1)–C(4)	1.446(18)	1.43
C(1)–N(1)	1.359(16)	1.35
N(2)–C(3)	1.406(17)	1.37
C(3)–C(2)	1.35(2)	1.35
C(2)–N(1)	1.385(18)	1.37
I(1)–Pd–C(4)′	95.6(3)	95
C(4)–Pd–I(2)	84.4(3)	85
Pd–C(4)–C(1)	116.5(9)	115
C(4)–C(1)–N(1)	125.7(13)	127
C(2)–N(1)–C(1)	107.7(12)	110
N(1)–C(2)–C(3)	109.2(13)	107
C(3)–C(2)–N(2)	105.5(13)	107
C(3)–N(2)–C(1)	109.5(12)	110
N(2)–C(1)–N(1)	107.9(11)	106

A good agreement was found between the experimental and calculated bond lengths and angles in **5**, demonstrating that DFT can predict accurately the structure of **3** and that the level of modelling was appropriate. The square-planar geometry around Pd strongly suggests a Pd^{II} complex in which the $CH_2CN_2(CH_3)_2C_2H_2$ ligand behaves as an ylide on coordination rather than as an olefin. The structural arrangement around C(4) is intermediate between sp^2 and sp^3 and somewhat closer to sp^2. The angles [°] in the complex are: H–C(4)–Pd 102, H–C(4)–H 110, C(1)–C(4)–Pd 116, H–C(4)–C(1) 113.

The neutral uncomplexed ligand $CH_2CN_2(CH_3)_2C_2H_2$ optimised to a conventional olefin structure with an *exo* C–C bond length of 1.37 Å (relaxed structure). The HOMO and HOMO-1 (Figure 4) contribute to the π component of the *exo* C=C bond. Distortion to the structure of the ligand in the optimised Pd complex (prepared structure) involves lengthening the *exo* C–C distance to 1.43 Å and pyramidalising the *exo* CH_2 group. Key structural parameters are compared in Figure 4. The HOMO and HOMO-1 of the distorted ligand retain some *exo* C–C π-bonding character. The high probability density of the HOMO on the *exo* C4 atom leads to coordination through this to the Pd rather than an η^2 coordination commonly found for most olefins. In addition, the C1–N distances shorten from 1.40 Å in the relaxed ligand to 1.37 Å in the complexed ligand, which provides evidence for the introduction of a delocalised positive charge into the imidazole ring upon coordination. Furthermore, in the relaxed ligand the Hirshfeld charge on C4 is –0.23, and this increases slightly to –0.27 in the complexed ligand, which is consistent with a change in charge on the imidazole ring.

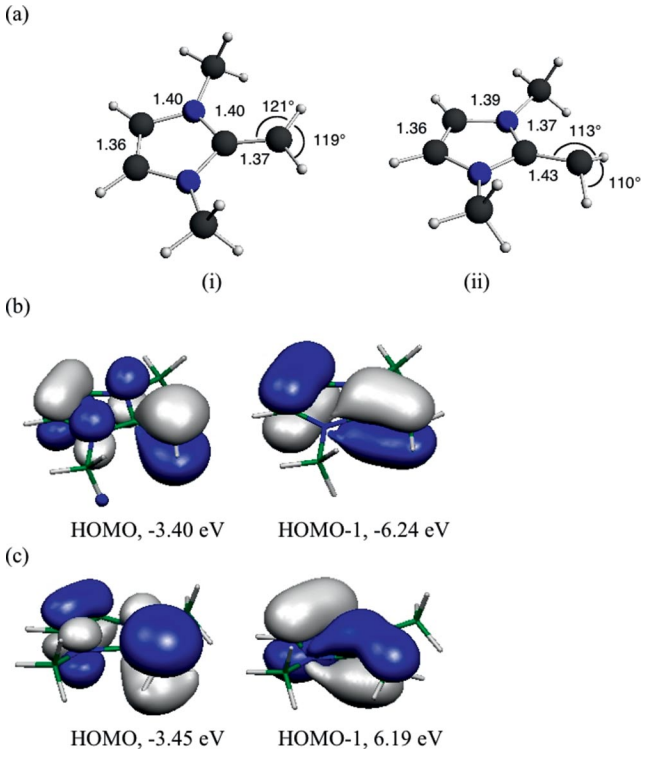

Figure 4. (a) Structural details for $CH_2CN_2(CH_3)_2C_2H_2$: (i) the optimised structure of the ligand; (ii) the ligand structure adopted in **5**. HOMO and HOMO-1, isosurfaces and energies of $CH_2CN_2(CH_3)_2C_2H_2$ in (b) the ground-state structure; (c) the structure when coordinated in **5**.

A fragment analysis was conducted within C_{2v} symmetry, in which **5** was separated into three fragments: a Pd fragment, the two neutral $CH_2CN_2(CH_3)_2C_2H_2$ groups and a neutral I_2 (I···I) fragment. The energy decomposition from the fragment analysis showed that over 92% of the orbital interaction came from orbitals of A_1 symmetry. The Pd $4d_{xy}$, $4d_{xz}$ and $4d_{yz}$ were effectively fully occupied. The upper orbitals of A_1 symmetry are shown in Figure 5. The HOMO is a localised d_{y^2} orbital completing the set of four occupied d orbitals, which is consistent with the square planar structure and a formal d^8 configuration for Pd^{II}.

The fragment analysis (Table 2) also indicates that linear combinations of the HOMO-1 and HOMO (Figure 5) of the $(CH_2CN_2(CH_3)_2C_2H_2)$ ligands interact with the Pd centre through a σ-interaction to form orbitals $22a_1$ and $20a_1$ of **5**. The LUMO, $25a_1$, is formed by an antibonding inter-

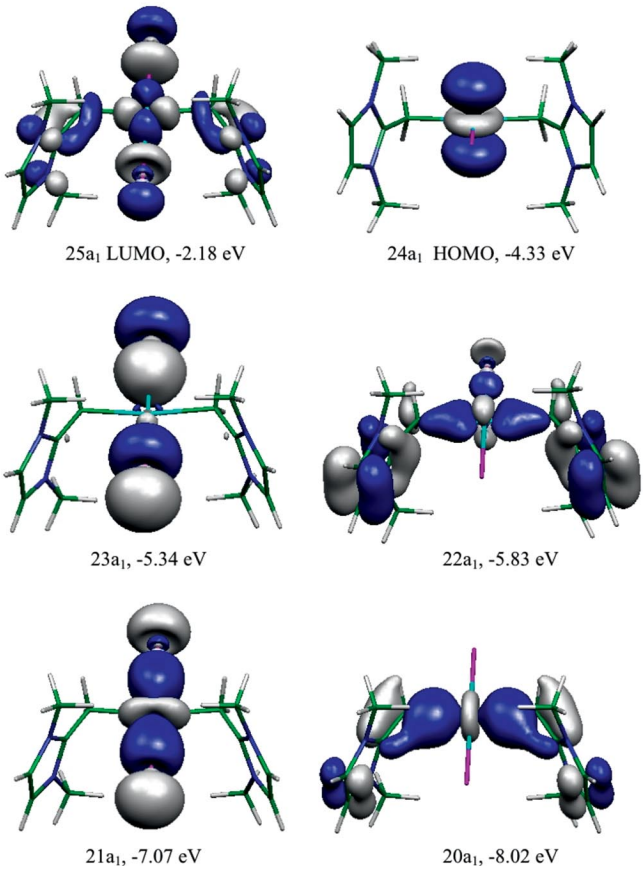

Figure 5. Isosurfaces and energies of selected orbitals of **5** of A_1 symmetry.

action of the $4d_{x^2-z^2}$ orbital with the σ donor orbitals of the I atoms and the $(CH_2CN_2(CH_3)_2C_2H_2)$ ligands. The carbons (C1) in the $(CH_2CN_2(CH_3)_2C_2H_2)_2$ ligands in **5** are stabilised not only through π-donation from the p orbitals of the nitrogen atoms of the imidazole rings but also through π-donation from the p orbitals of the carbon atoms bonded to the Pd (C4), resulting in the retention of some of the *exo* C–C π bonding character mentioned earlier.

Table 2. Contributions (>5%) from fragment orbitals to the MOs 20a$_1$ and 22a$_1$ of **5**.

Fragment orbital	Ligand HOMO	Ligand HOMO-1	Pd $d_{x^2-y^2}$	Pd d_{z^2}
MO 22a$_1$	33%	42%		12%
MO 20a$_1$	17%	50%	16%	5%

Hirshfeld charge analysis indicates that the carbon atoms bonded to the metal centre, C4 and C4′, are nucleophilic (Hirshfeld charges on both atoms are –0.27), while the carbene atoms, C1 and C1′, are only slightly electrophilic (0.09). Moreover, there is a positive charge on the palladium centre (0.24) and negative charges on both of the iodide ligands (–0.23 and –0.33). This is reasonably consistent with our description of a Pd^{II} complex with four X type ligands, and two tethered cations to give a neutral species. The carbene atoms, C1 and C1′, are only slightly electrophilic, because the positive charge is delocalised across the imidazole rings.

Mechanistic Considerations

Detailed mechanistic investigations have been carried out by Hofmann et al. on reactions involving platinum compounds that are capable of activating C–Si bonds under mild conditions (Scheme 3).[13]

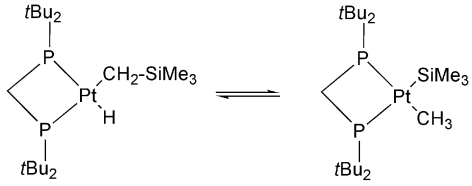

Scheme 3. Activation of C–Si bonds by platinum(II) compounds.

In the light of this work, a possible mechanism for the formation of **2**, **3**, palladium black and hexamethyldisilane (detected by mass spectrometry and ^1H and ^{13}C NMR spectroscopy in the reaction solution) is shown in Scheme 4.

In Scheme 4, the first step is the oxidative addition of (trimethylsilyl)methyl iodide to **1**, followed by dissociation of a carbene ligand, and subsequent attack of the electropositive silicon atom on the latter. The newly formed "Pd-CH_2" species quickly reacts with the electron-deficient imidazolium carbon atom, affording the heteroleptic Pd(TMS)(CH_2I*t*Bu)(I*t*Bu)I complex, which rearranges by ligand exchange to give the two corresponding symmetrical species. The Pd(TMS)(I*t*Bu)$_2$I loses I*t*Bu and dimerises to form **2**, while the Pd(TMS)(CH_2I*t*Bu)$_2$I reacts by an intermolecular exchange mechanism (see inset to Figure 4), previously reported for a number of palladium(II)(alkyl) or (aryl)halide type complexes,[11,14] to produce **3**, hexamethyldisilane and palladium black.

Conclusions

The reaction of Me_3SiCH_2I with [Pd(I*t*Bu)$_2$] results in carbon–silicon bond activation and formation of [Pd(Me_3-Si)(I*t*Bu)(μ-I)]$_2$ (**2**) and [Pd(CH_2I*t*Bu)I$_2$] (**3**). The bonding in **3** was investigated by using DFT methods. On the basis of both the crystal structure and theoretical analysis, we formulate **3** as a dianionic species with two tethered cations resulting in a neutral zwitterionic complex. The role of counterions in catalysis and polymerisation is often unclear, and the ability of **3** to act as a pre-catalyst will be investigated.

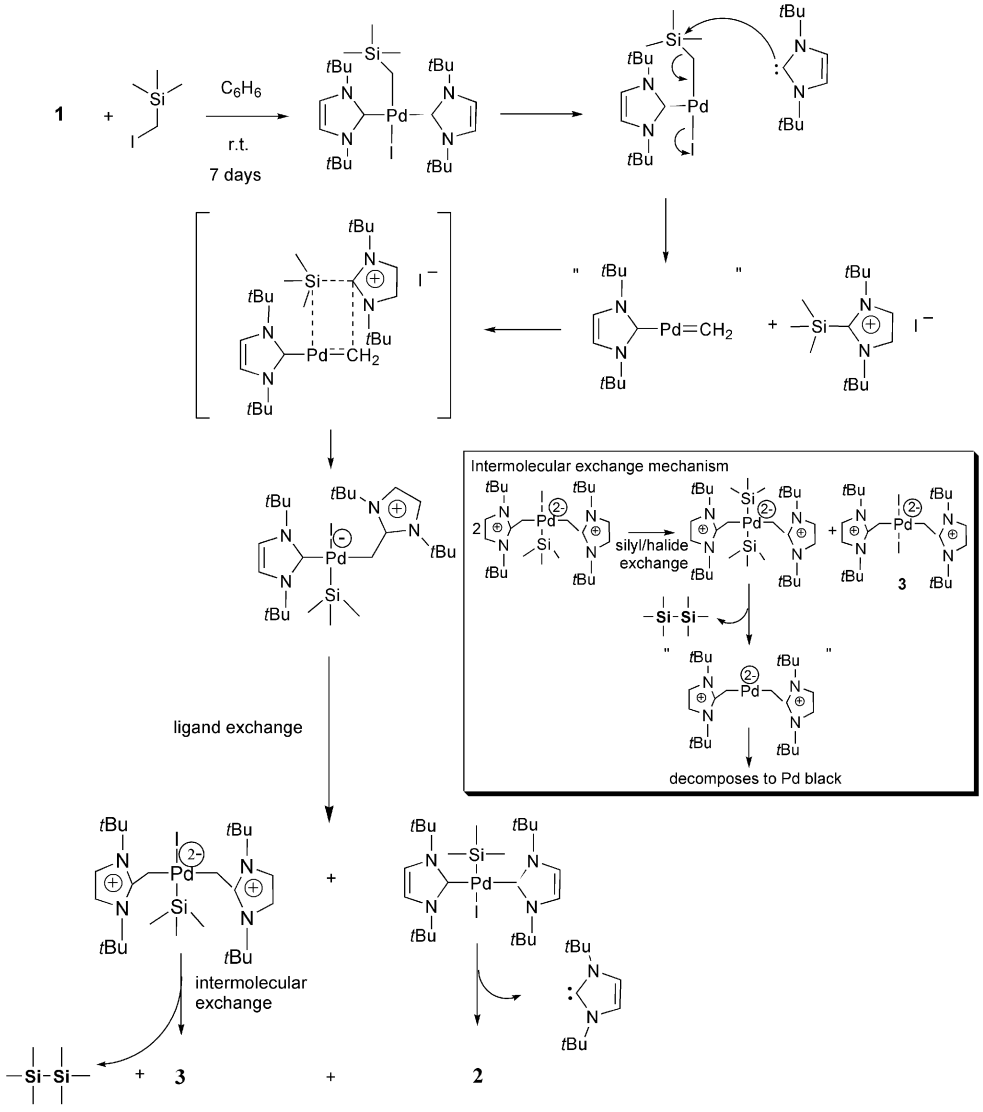

Scheme 4. Proposed mechanism.

Experimental Section

General Remarks: Unless otherwise stated, all manipulations were performed by using standard Schlenk line techniques under nitrogen or vacuum, or in a nitrogen atmosphere provided by an MBraun or a Miller Howe glove box (<2 ppm O_2/<1 ppm H_2O). Glassware was dried in a 150 °C oven, and Celite 545 filter aid was flame-dried in vacuo prior to use.

Solvents were purified by pre-drying prior to heating at reflux over a suitable drying agent in a solvent still under an atmosphere of dinitrogen. Once collected, the dried solvent was transferred into an ampoule, degassed and stored under argon (Table 3).

[D_3]Chloroform was purified by refluxing over calcium hydride, then vacuum-transferred to an ampoule and stored under dinitrogen in a glove box. [D_6]Benzene was purified by refluxing over potassium metal, then vacuum-transferred to an ampoule and stored under dinitrogen in a glove box

NMR spectra were recorded with a Bruker Avance 300DPX spectrometer, operating at 300.13 MHz for ^{1}H measurements and 75.47 MHz for ^{13}C measurements, or with a Bruker 500AMX operating at 500.13 MHz for ^{1}H measurements. ^{1}H and ^{13}C NMR spectra were referenced to the residual proton or carbon chemical shifts of the deuteriated solvent. Unless otherwise indicated, all spectra were recorded at 298 K. Coupling constants are reported in Hertz. Mass spectra (EI, FAB and GC-MS) were recorded with an Autospec instrument (electron ionisation at 70 eV). Elemental analyses were performed by the University of North London.

Table 3. Details of solvent purification.

Solvent	Drying agent	Stored over
Toluene	sodium	potassium mirror
Diethyl ether	sodium/potassium alloy	potassium mirror
Pentane	sodium/potassium alloy	potassium mirror
Petroleum ether	sodium/potassium alloy	potassium mirror
Benzene	potassium	potassium mirror
thf	potassium	4 Å molecular sieves
CH_2Cl_2	calcium hydride	4 Å molecular sieves
Chloroform	calcium hydride	4 Å molecular sieves

(Trimethylsilyl)methyl iodide and trimethylsilyl iodide (TMSI) were purchased from Aldrich and dried with activated 3-Å molecular

sieves, degassed and vacuum-transferred into ampoules equipped with greaseless stopcocks. Pd(I*t*Bu)$_2$ (**1**) was prepared by the literature procedure.[15]

Synthesis of [(I*t*Bu)Pd(TMS)(μ-I)]$_2$ (2) and Pd(CH$_2$I*t*Bu)$_2$I$_2$ (3) by Using (Trimethylsilyl)methyl Iodide: Compound **1** (0.080 g, 0.17 mmol) was dissolved in benzene (5 mL), and (trimethylsilyl)-methyl iodide (2.5 equiv., 63.20 μL) was added by a microlitre syringe. Over a period of 3 d, the initially green solution gradually turned to deep red, and palladium black was deposited; the solution was filtered, and yellow and red crystals appeared in the filtrate after a further 4 d. The crystals were isolated by filtering the mother solution through a thin filter cannula and by washing the resultant crystalline solid with pentane. X-ray analysis of a yellow crystal revealed the structure of complex **2**, while the X-ray analysis of a red crystal revealed the structure of complex **3**. The poor solubility of the two compounds, **2** and **3**, in a number of solvents, such as Et$_2$O, petroleum/diethyl ether, thf and dioxane, made their separation impossible. The total yield of **2** and **3** was ca. 65% based on palladium. Compounds **2** and **3** were found to be both partially soluble in [D$_6$]chloroform; therefore, ^{1}H NMR and ^{13}C NMR spectroscopy were carried out on the mixture of the two complexes (see below).

[(I*t*Bu)Pd(TMS)(μ-I)]$_2$ (2): ^{1}H NMR ([D$_6$]chloroform): δ = 7.18 (s, 4 H, CH=CH), 1.70 [s, 36 H, C(CH$_3$)$_3$], 0.05 [s, 18 H, Si(CH$_3$)$_3$] ppm. ^{13}C NMR {^{1}**H**} ([D$_6$]chloroform): δ = 174.9 (Pd-C$_{carbene}$), 118.7 (*C*H=*C*H), 59.5 [*C*(CH$_3$)], 33.2 [C(*C*H$_3$)], 5.0 [Si(*C*H$_3$)$_3$] ppm.

Pd(CH$_2$I*t*Bu)$_2$I$_2$ (3): ^{1}H NMR ([D$_6$]chloroform): δ = 7.52 (s, 4 H, CH=CH), 3.02 (s, 4 H, CH$_2$-Pd), 1.69 (s, 36 H, CH$_3$) ppm. ^{13}C{^{1}H} NMR ([D$_6$]chloroform): δ = 168.0 (C$_{ring}$), 115.1 (*C*H=*C*H), 119.0 (*C*H$_2$-Pd), 59.4 [*C*(CH$_3$)$_3$], 30.4 (*C*H$_3$) ppm.

Synthesis of [(I*t*Bu)Pd(TMS)(μ-I)]$_2$ (2) by Using Trimethylsilyl Iodide: Pd(I*t*Bu)$_2$ (**1**) (0.02 g; 0.04 mmol) was dissolved in [D$_6$]benzene (0.6 mL) in an NMR tube equipped with a greaseless stopcock, and TMSI (0.08 mmol; 11.43 μL) was added by a microlitre syringe. ^{1}H NMR spectra were acquired regularly until the reaction went to completion.

[(I*t*Bu)Pd(TMS)(μ-I)]$_2$ (2): ^{1}H NMR ([D$_6$]benzene): δ = 6.57 (s, 4 H, CH=CH); 1.86 [s, 36 H, C(CH$_3$)$_3$], 0.57 [s, 18 H, Si(CH$_3$)$_3$] ppm.

Crystal Structure Determination of 2 and 3: Crystals of **2** and **3** were mounted in oil, and data were collected with an Enraf–Nonius KAPPA CCD diffractometer equipped with a graphite-monochromated Mo-K_α radiation source and an area detector, at 173(2) K. The structures were solved by using the WinGX program package, with absorption correction with MULTISCAN and refinement with SHELXL-97. All non-hydrogen atoms were refined anisotropically by full-matrix least-squares. Hydrogen atoms were refined in riding mode with U_{iso}(H) = 1.2 U_{eq}(C) or 1.5 U_{eq}(C) for methyl groups. Crystallographic and experimental details are summarised in Table 4. CCDC-703468 and -703469 (for complexes **2** and **3**, respectively) contain the supplementary crystallographic data for this paper. These data can be obtained free of charge from The Cambridge Crystallographic Data Centre via www.ccdc.cam.ac.uk/data_request/cif.

Computational Studies: Quantum chemical calculations were performed by using density functional methods of the Amsterdam Density Functional (Versions ADF2004.01 and ADF2007.01) package.[16–19] In the calculations, the generalised gradient approximation was employed by using the local density approximation of Vosko, Wilk and Nusair,[20] together with the nonlocal-exchange correction by Becke[21] and the nonlocal-correlation corrections by Perdew.[22] TZP basis sets were used with triple-ξ accuracy sets of Slater-type orbitals, polarisation functions being added to all atoms. Relativistic corrections were made by using the ZORA (zero-order relativistic approximation) formalism.[23–27] The core electrons were frozen up to 1s for C and N, 4p for I and 3d for Pd. All quoted electronic structure data from optimised structures use an integration grid of 4.0 and have gradient corrections applied after the SCF cycles. Fragment analyses use the MOs of the chosen

Table 4. Crystal data and structure refinement for **2** and **3**.

	2	**3**
Empirical formula	$C_{28}H_{58}I_2N_4Pd_2Si_2$	$C_{24}H_{44}I_2N_4Pd{\cdot}C_6D_6$
Formula weight	973.56	832.94
Temperature	173(2) K	173(2) K
Crystal system	hexagonal	monoclinic
Space group	$P6_122$ (No.178)	$C2/c$ (No.15)
a [Å]	9.7311(3)	12.4498(9)
b [Å]	9.7311(3)	22.9129(15)
c [Å]	69.2802(19)	12.3461(8)
α [°]	90°	90°
β [°]	90°	104.942(4)°
γ [°]	120°	90°
Volume [Å^3]	5681.5(3)	3402.8(4)
Z	6	4
Density (calculated) [Mg m^{-3}]	1.71	1.63
Absorption coefficient [mm^{-1}]	2.67	2.38
θ range for data collection	3.58 to 26.02°	3.51 to 22.96°
Reflections collected	14921	8666
Independent reflections	3604 [R(int) = 0.054]	2311 [R(int) = 0.078]
Reflections with $I > 2\sigma(I)$	3411	1592
Refinement method	Full-matrix least-squares on F^2	Full-matrix least-squares on F^2
Data/restraints/parameters	3604/30/170	2311/0/169
Goodness-of-fit on F^2	1.275	1.061
Final R indices [$I > 2\sigma(I)$]	$R1$ = 0.031, $wR2$ = 0.092	$R1$ = 0.072, $wR2$ = 0.142
R indices (all data)	$R1$ = 0.037, $wR2$ = 0.107	$R1$ = 0.112, $wR2$ = 0.160
Largest diff. peak/hole [e Å^{-3}]	1.40 and –1.57 (near I atoms)	2.40 and –0.94 (near I atoms)

fragments as the basis set for the molecular calculation. Initial spin-restricted calculations are carried out on the fragments with the geometry that they have in the molecule; thus the fragments are in a prepared singlet state. Neutral fragments were chosen, as this assisted in drawing up the MO diagrams.

Acknowledgments

We thank the Engineering and Physical Sciences Research Council for financial support and (the late) Dr. Tony Avent for assistance with the NMR spectroscopic studies.

[1] R. H. Crabtree, R. Kulawiecz, *Coord. Chem. Rev.* **1990**, *99*, 89.
[2] a) H. C. Clark, M. Hampden-Smith, *Coord. Chem. Rev.* **1987**, *79*, 229; b) H. Hayashi, T. Yamashita, M. Kobayashi, T. Tanaka, M. Goto, *J. Am. Chem. Soc.* **1988**, *110*, 4417; c) J. K. Stille, K. S. Y. Lau, *J. Am. Chem. Soc.* **1976**, *98*, 5841; d) C. Eaborn, R. W. Griffiths, A. Pidcock, *J. Organomet. Chem.* **1982**, *225*, 331; e) A. A. Zlota, F. Frolow, D. Milstein, *J. Chem. Soc., Chem. Commun.* **1989**, 1826.
[3] P. Braunstein, M. Knorr, *J. Organomet. Chem.* **1995**, *500*, 28.
[4] I. Ojima, Z. Li, J. Zhu, *The Chemistry of Organic Silicon Compounds* John Wiley and Sons, Chichester, **1998**.
[5] a) J. Y. Corey, X. Zhu, T. C. Bedard, L. D. Lange, *Organometallics* **1991**, *10*, 924; b) J. F. Harrod, T. Ziegler, V. Tschinke, *Organometallics* **1990**, *9*, 897; c) E. Hengge, M. Weinberger, *J. Organomet. Chem.* **1992**, *441*, 397.
[6] a) I. Ojima, P. Ingallina, R. J. Donovan, N. Clos, *Organometallics* **1991**, *10*, 38; b) F. Monteil, I. Matsuda, H. Alper, *J. Am. Chem. Soc.* **1995**, *117*, 4419.
[7] K. Yamamoto, H. Okinoshino, Y. Nagai, *J. Organomet. Chem.* **1970**, *23*, C7.
[8] H. Okinoshima, K. Yamamoto, M. Kumada, *J. Am. Chem. Soc.* **1972**, *94*, 9263.
[9] a) S. Shimada, M. Tanaka, *Coord. Chem. Rev.* **2006**, 250, 991; b) M. Murakami, T. Oshida, Y. Y. Ito, *Organometallics* **1994**, *13*, 2900; c) F. Ozawa, M. Sugawara, T. Hayashi, *Organometallics* **1994**, *13*, 3237; d) M. D. Curtis, J. Greene, *J. Am. Chem. Soc.* **1978**, *100*, 6362; e) U. Schubert, C. Miiller, *J. Organomet. Chem.* **1989**, *373*, 165; f) M. A. Guerra, R. J. Lagow, *J. Chem. Soc., Chem. Commun.* **1990**, 65; g) Y. Pan, J. T. Mague, M. Fink, *Organometallics* **1992**, *11*, 3495; h) T. K. Woo, G. Pioda, U. Rothlisberger, A. Togni, *Organometallics* **2000**, *19*, 2144; i) Y. J. Lee, J. D. Lee, S. J. Kim, S. Keum, J. J. Ko, I. H. Suh, M. Cheong, S. O. Kang, *Organometallics* **2004**, *23*, 203.
[10] N. Chatani, N. Amishiro, S. Murai, *J. Am. Chem. Soc.* **1991**, *113*,7778.
[11] O. Esposito, A. K. de K. Lewis, P. B. Hitchcock, S. Caddick, F. G. N. Cloke, *Chem. Commun.* **2007**, 1157.
[12] F. Ozawa, M. Sugawara, K. Hasebe, T. Hayashi, *Inorg. Chim. Acta* **1999**, *296*, 19.
[13] P. Hofmann, H. Heiss, P. Neiteler, G. Miiller, J. Lachmann, *Angew. Chem. Int. Ed. Engl.* **1990**, *29*, 880.
[14] D. S. McGuinness, K. J. Cavell, *Organometallics* **1999**, *18*, 1596.
[15] S. Caddick, F. G. N. Cloke, G. K. B. Clentsmith, P. B. Hitchcock, D. McKerrecher, L. R. Titcomb, M. R. V. Williams, *J. Organomet. Chem.* **2001**, *617*, 635.
[16] G. te Velde, F. M. Bickelhaupt, S. A. J. van Gisbergen, C. Fonseca Guerra, E. J. Baerends, J. G. Snijders, T. Ziegler, *J. Comput. Chem.* **2001**, *22*, 931–967.
[17] C. Fonseca Guerra, J. G. Snijders, G. te Velde, E. J. Baerends, *Theor. Chem. Acc.* **1998**, *99*, 391.
[18] *ADF* 2004.01, SCM, Theoretical Chemistry, Vrije Universiteit, Amsterdam, **2004**.
[19] *ADF* 2007.01, SCM, Theoretical Chemistry, Vrije Universiteit, Amsterdam, **2007**.
[20] S. H. Vosko, L. Wilk, M. Nusair, *Can. J. Phys.* **1980**, *58*, 1200–1211.
[21] A. D. Becke, *Phys. Rev. A: At. Mol. Opt. Phys.* **1988**, *38*, 3098–3100.
[22] J. P. Perdew, W. Yue, *Phys. Rev. B* **1986**, *33*, 8800.
[23] E. Vanlenthe, E. J. Baerends, J. G. Snijders, *J. Chem. Phys.* **1993**, *99*, 4597–4610.
[24] E. Vanlenthe, E. J. Baerends, J. G. Snijders, *J. Chem. Phys.* **1994**, *101*, 9783–9792.
[25] E. Vanlenthe, E. J. Baerends, J. G. Snijders, *J. Chem. Phys.* **1996**, *105*, 6505–6516.
[26] E. Vanlenthe, R. VanLeeuwen, E. J. Baerends, J. G. Snijders, *J. G. Int. J. Quantum Chem.* **1996**, *57*, 281–293.
[27] E. Vanlenthe, A. Ehlers, E. J. Baerends, *J. Chem. Phys.* **1999**, *110*, 8943–8953.

Received: November 27, 2008
Published Online: March 5, 2009

